Engineering Applications of Artificial Intelligence 42 (2015) 1–15

Contents lists available at ScienceDirect

Engineering Applications of Artificial Intelligence

journal homepage: www.elsevier.com/locate/engappai

Gain estimation of nonlinear dynamic systems modeled by an FBFN and the maximum output scaling factor of a self-tuning PI fuzzy controller

Phuong D. Ngo, Yung C. Shin *

School of Mechanical Engineering, Purdue University, West Lafayette, Indiana, USA

ARTICLE INFO

Article history:
Received 28 April 2014
Received in revised form
27 February 2015
Accepted 6 March 2015

Keywords:
Stability
Fuzzy control
Nonlinear systems
Self-tuning control
Small gain theorem

ABSTRACT

This paper proposes new techniques to calculate the dynamic gains of nonlinear systems represented by fuzzy basis function network (FBFN) models. The dynamic gain of an FBFN can be approximated by finding the maximum of norm values of the locally linearized systems or by solving a non-smooth optimal control problem. From the proposed gain calculation techniques, a novel adaptive multilevel fuzzy controller (AMLFC) with a maximum output scaling factor is presented. To guarantee the system stability, a stability condition is derived, which only requires that the output scaling factor of the AMLFC be bounded. Therefore, this paper provides a systematic and simple design practice for controlling nonlinear systems by using an AMLFC. The AMLFC is simulated in a tower crane control system. Simulation results show that AMLFC is not only robust but also provides improved transient performances compared with the robust adaptive fuzzy controller.

1. Introduction

Fuzzy controllers are constructed based on heuristic rules and "expert knowledge" derived from physical systems. Early fuzzy control papers did not provide mathematical stability analysis or proofs of the control systems (Sala, 2013). However, the stability of a fuzzy control system is very important in the controller design process to guarantee desired performance and safety in the plant operations.

The applications of the small gain theorem (Jiang et al., 2010; Yang, 2005) and the passivity theory (Xu and Shin, 2005) in fuzzy control systems show great advantages compared to other stability methods. These stability theories do not require an exact mathematical representation of the plant and, therefore, they can be applied to nonlinear systems with unknown mathematical models. With the small gain theorem, Chen and Ying (1993) demonstrated how the parameters of a proportional-integral (PI) fuzzy controller could be chosen to ensure the input-output stability of a nonlinear system. However, the stability criteria developed are only limited to a certain type of fuzzy controllers with two input and three output membership functions. Since Chen and Ying (1993) divided the stability problem according to the locations of the error and the time rate of change of the error with respect to zero, the complexity of the problem would exponentially increase if the number of input and output membership functions increases. In the current work, the stability analysis is conducted based on the location of the error and the time rate of change of the error with respect to the activated membership functions. The results, therefore, can be applied to fuzzy controllers with any number of input and output membership-functions.

Since mathematical models for nonlinear systems cannot always be easily obtained, fuzzy basis function network (FBFN) models were adopted in many applications (Chiang et al., 2012; Lee and Shin, 2001; Leng et al., 2005) to represent the relationship between the inputs and outputs of the systems. With a set of input and output data, Wang and Mendel (1992) showed that any nonlinear system can be approximated by an FBFN model. However, controllers implemented with FBFN models are still limited, owing to a lack of stability analysis. Due to the nonlinearity characteristics of the FBFN, the small gain theorem is the most appropriate approach to finding the stability region in this case. Therefore, obtaining the dynamic gain from an FBFN model is the first step towards achieving the stability condition for nonlinear fuzzy control systems.

* Corresponding author. Tel.: +1 765 49 49775.
E-mail address: shin@purdue.edu (Y.C. Shin).

http://dx.doi.org/10.1016/j.engappai.2015.03.004

In many applications where heuristic information for designing a fuzzy controller is not sufficient, the parameters of a fuzzy controller can be computed offline by using input and output data (Chen et al., 2009; Lin and Xu, 2006; Mingzhi et al., 2009). Ying (1994) introduced a method for obtaining the parameters of a PI fuzzy controller by tuning a linear PI controller. However, the global stability of the control system could not be guaranteed, since Ying's method only showed local stability around the equilibrium points, nor could it determine the size of the region of local stability. When there are disturbances and time-varying parameters, online adaptation of control parameters based on data gathered in real-time would be more effective. Li and Tong (2003) proposed a hybrid control system, which consists of a state observer, an adaptive fuzzy mechanism, an H^{∞} control and a sliding mode control. Boubakir et al. (2011) used a different approach to tune the parameters of a proportional-integral-derivative (PID) controller for multi-input multi-output (MIMO) dynamic systems by minimizing the error between an ideal controller and the PID controller. However, the controllers developed by both Li and Tong (2003) and Boubakir et al. (2011) can only be applied to a certain class of nonlinear dynamic systems where the input is represented by a linear term in the system's mathematical model. Pellegrinetti and Bentsman (1996) offer an example of nonlinear systems that cannot be represented in this form. Furthermore, stability conditions for the controllers presented in these papers must be calculated based on the upper bounds of the model functions. These values are difficult to obtain in many cases where the system models are unknown. In the current work, since an FBFN is used as a representation of nonlinear systems, the stability condition depends only on the dynamic gain that can be computed directly from the FBFN's parameters.

Different studies have been conducted to improve the performance of fuzzy controllers. Haj-Ali and Ying (2004) and Arya (2007) have analyzed the structures of PI fuzzy controllers and found the effects of nonlinear and asymmetrical input sets on the performance of the controllers. Chen and Ying (1993) and Haj-Ali and Ying (2004) demonstrated that fuzzy PI and PID controllers could be treated as nonlinear PI and PID controllers. Mudi and Pal (1999) presented a method to tune the output-scaling factors of fuzzy controllers by using the error and the time rate of change of the error signals. However, this method is based only on an intuitive analysis of the desired performances to keep the system stable; no mathematical stability analysis was provided in their work. In Woo et al. (2000), a PID fuzzy controller was proposed with self-tuning algorithms for both input and output scaling factors, but lacked a systematic stability analysis. The multilevel fuzzy controller (MLFC) system was proposed by Xu and Shin (2005), wherein the controller has an adaptive mechanism designed to tune the output membership functions based on the system outputs. Although the MLFC has been successfully utilized in different applications (Davis et al., 2011; Ngo and Shin, 2012), the controller still has some limits when dealing with time-variant systems such as sectorial restrictions on membership functions.

The current work proposes a novel method to estimate the dynamic gain of a nonlinear system and discusses the design process for a new MLFC with an adaptive mechanism for the output scaling factor. The design can improve the transient performance of control systems while eliminating the need for initial parameter tuning. The stability analysis is conducted based on the small gain theorem and uses the dynamic gain of the nonlinear system to provide the maximum bound of the MLFC's output scaling factor for system stability.

2. Dynamic gain estimation of nonlinear dynamic systems modeled by FBFNs

The stability analysis of a nonlinear fuzzy control system based on the small gain theorem requires an estimation of the dynamic gain of the plant. Two methods are provided in this section to calculate the gain of an FBFN system. In the first method, the dynamic gain can be approximated by finding the maximum of the norm values of the locally linearized systems. This method provides an effective technique for FBFN models with a large number of fuzzy rules, since the estimation can be done based on experimental data. The second method provides an analytical computation technique of the dynamic gain based on a non-smooth optimal control problem. To simplify mathematical analysis, only nonlinear systems with single input and single output (SISO) are considered in this paper. However, the technique can be easily expanded to MIMO systems by applying the same procedure for each individual input and output pair.

2.1. Local linear model of a nonlinear systems represented by FBFNs

This subsection provides a method for obtaining the local linear model of a nonlinear system from its FBFN model. For a SISO nonlinear system, an FBFN model can be constructed from the input and output data through a set of l fuzzy rules, where the ith rule R^i is described as following:

$$\begin{aligned} &\mathrm{R}^i: \quad \text{If } u(k-1)=A_1^i \text{ AND } u(k-2)=A_2^i \text{ AND } \ldots\text{AND } u(k-m)=A_m^i \text{ AND} \\ &y(k-1)=B_1^i \text{ AND } y(k-2)=B_2^i \cdots\text{AND } y(k-n)=B_n^i \\ &\text{then } y(k)=b^i \end{aligned} \tag{1}$$

where $u(k)$ is the input and $y(k)$ denotes the output of the nonlinear system at time instance k, m and n represent the system orders of the input and the output,

$A_1 \ldots A_m$ and $B_1 \ldots B_n$ are fuzzy membership sets, and

b represents a singleton function of the output.

Assume that the output of the FBFN model at initial condition is zero, by using singleton fuzzification, product inference and centroid defuzzification methods, the FBFN model can be represented by the following state space equations:

$$\begin{aligned} &\mathbf{x}(k)=\mathbf{f}(\mathbf{x}(k-1),\mathbf{u}(k-1)) \\ &y(k)=\mathbf{c}^T\mathbf{x}(k) \end{aligned} \tag{2}$$

where

$$\mathbf{x}(k)=\left[y(k),\ldots y(k-n+1)\right]^T,\ \mathbf{u}(k)=\left[u(k),\ldots,u(k-m+1)\right]^T,\ \mathbf{x}(0)=[0,\ 0,\ \ldots,0]^T, \tag{3}$$

$$\mathbf{f}(\mathbf{x}(k-1),\mathbf{u}(k-1)) = \begin{bmatrix} f(\mathbf{x}(k-1),\mathbf{u}(k-1)) \\ y(k-1) \\ \vdots \\ y(k-n+1) \end{bmatrix}, \quad \mathbf{c} = [1,0,\ldots 0]^T \tag{4}$$

The nonlinear mapping $f: \mathbf{u} \subset \Re^m, \mathbf{x} \subset \Re^n \rightarrow y \subset \Re$ in Eq. (4) is described through the fuzzification process as follows:

$$f(\mathbf{x},\mathbf{u}) = \frac{\sum_{i=1}^{l}\left(b^i \cdot \left\{\prod_{t_u=1}^{m} \mu_{A^i_{t_u}}[u(k-t_u)]\right\} \cdot \left\{\prod_{t_y=1}^{n} \mu_{B^i_{t_y}}[y(k-t_y)]\right\}\right)}{\sum_{i=1}^{l}\left(\left\{\prod_{t_u=1}^{m} \mu_{A^i_{t_u}}[u(k-t_u)]\right\} \cdot \left\{\prod_{t_y=1}^{n} \mu_{B^i_{t_y}}[y(k-t_y)]\right\}\right)}, \tag{5}$$

where $\mu_{A^i_{t_u}}[u(k-t_u)]$ and $\mu_{A^i_{t_y}}[y(k-t_y)]$ are input and output membership functions represented by:

$$\mu_{A^i_{t_u}}[u(k-t_u)] = \exp\left\{-\frac{1}{2}\left[\frac{u(k-t_u)-m^i_{t_u}}{\sigma^i_{t_u}}\right]^2\right\}, \quad \mu_{A^i_{t_y}}[y(k-t_y)] = \exp\left\{-\frac{1}{2}\left[\frac{u(k-t_y)-m^i_{t_y}}{\sigma^i_{t_y}}\right]^2\right\} \tag{6}$$

m^i_t and σ^i_t are real-valued parameters that represent the center and width of each Gaussian MF; $t_u = 1\ldots\, m$ and $t_y = 1\ldots n$ are the numbers of delay terms of the system input and output, respectively; and l is the number of the FBFN's rules.

When the states of the system are around a certain trajectory described by $\mathbf{x}_0$ and $\mathbf{u}_0$:

$$\begin{aligned} &\mathbf{x}_0(k-1) = [y_0(k-1),\ldots,y_0(k-n)], \quad \mathbf{u}_0(k-1) = [u_0(k-1),\ldots,u_0(k-m)] \\ &\mathbf{x}_0(k) = \mathbf{f}(\mathbf{x}_0(k-1),\mathbf{u}_0(k-1)), \ \ \mathbf{x}_0(0) = [0,\ 0,\ \ldots,0]^T \end{aligned} \tag{7}$$

the time-varying linear model of the nonlinear system respresented by Eq. (2) can be obtained as follows:

$$\begin{aligned} \mathbf{x}(k) &= \mathbf{f}(\mathbf{x}_0(k-1),\mathbf{u}_0(k-1)) + \mathbf{A}(\mathbf{x}_0(k-1),\mathbf{u}_0(k-1))[\mathbf{x}(k-1)-\mathbf{x}_0(k-1)] \\ &\quad + \mathbf{B}(\mathbf{x}_0(k-1),\mathbf{u}_0(k-1))[\mathbf{u}(k-1)-\mathbf{u}_0(k-1)] \\ y(k) &= \mathbf{c}^T\mathbf{x}(k) \end{aligned} \tag{8}$$

where

$$\mathbf{A}(\mathbf{x}_0,\mathbf{u}_0) = \begin{bmatrix} a_1 & a_2 & \ldots & a_n \\ 0 & 1 & \ldots & 0 \\ \vdots & & & \\ 0 & 0 & \ldots & 1 \end{bmatrix}, \quad \mathbf{B}(\mathbf{x}_0,\mathbf{u}_0) = \begin{bmatrix} b_1 & b_2 & \ldots & b_m \\ 0 & 1 & \ldots & 0 \\ \vdots & & & \\ 0 & 0 & \ldots & 1 \end{bmatrix}, \quad \mathbf{x}(0) = [0,\ 0,\ \ldots,0]^T \tag{9}$$

The matrices **A** and **B** are constructed from the linearizing coefficients a_{t_y} and b_{t_u} ($t_y = 1\ldots n$ and $t_u = 1\ldots\, m$), which can be calculated by the following formulas (Xu and Shin, 2011):

$$\begin{aligned} a_{t_y} = \left.\frac{\partial f}{\partial y(k-t_y)}\right|_{\mathbf{x}=\mathbf{x}_0,\,\mathbf{u}=\mathbf{u}_0} &= -\frac{\sum_{i=1}^{l}\left\{b^i \cdot \left[\prod_{t_u=1}^{m} \mu_{A^i_{t_u}}[u(k-t_u)]\right] \cdot \left[\prod_{t_y=1}^{n} \mu_{B^i_{t_y}}[y(k-t_y)]\right]\left[\frac{y(k-t_y)-c^i_{t_y}}{(\sigma^i_{t_y})^2}\right]\right\}}{\sum_{i=1}^{l}\left[\left\{\prod_{t_u=1}^{m} \mu_{A^i_{t_u}}[u(k-t_u)]\right\} \cdot \left\{\prod_{t_y=1}^{n} \mu_{B^i_{t_y}}[y(k-t_y)]\right\}\right]} \\ &+ \frac{\sum_{i=1}^{l}\left\{b^i \cdot \left[\prod_{t_u=1}^{m} \mu_{A^i_{t_u}}[u(k-t_u)]\right] \cdot \left[\prod_{t_y=1}^{n} \mu_{B^i_{t_y}}[y(k-t_y)]\right]\right\} \cdot \left\{\sum_{i=1}^{l}\left\{\left\{\prod_{t_u=1}^{m} \mu_{A^i_{t_u}}[u(k-t_u)]\right\} \cdot \left\{\prod_{t_y=1}^{n} \mu_{B^i_{t_y}}[y(k-t_y)]\right\}\left[\frac{y(k-t_y)-c^i_{t_y}}{(\sigma^i_{t_y})^2}\right]\right\}\right\}}{\left\{\sum_{i=1}^{l}\left[\left\{\prod_{t_u=1}^{m} \mu_{A^i_{t_u}}[u(k-t_u)]\right\} \cdot \left\{\prod_{t_y=1}^{n} \mu_{B^i_{t_y}}[y(k-t_y)]\right\}\right]\right\}^2} \end{aligned} \tag{10}$$

and

$$\begin{aligned} b_{t_u} = \left.\frac{\partial f}{\partial u(k-t_u)}\right|_{\mathbf{x}=\mathbf{x}_0,\,\mathbf{u}=\mathbf{u}_0} &= -\frac{\sum_{i=1}^{l}\left\{b^i \cdot \left[\prod_{t_u=1}^{m} \mu_{A^i_{t_u}}[u(k-t_u)]\right] \cdot \left[\prod_{t_y=1}^{n} \mu_{B^i_{t_y}}[y(k-t_y)]\right]\left[\frac{u(k-t_u)-c^i_{t_u}}{(\sigma^i_{t_u})^2}\right]\right\}}{\sum_{i=1}^{l}\left[\left\{\prod_{t_u=1}^{m} \mu_{A^i_{t_u}}[u(k-t_u)]\right\} \cdot \left\{\prod_{t_y=1}^{n} \mu_{B^i_{t_y}}[y(k-t_y)]\right\}\right]} \\ &+ \frac{\sum_{i=1}^{l}\left\{b^i \cdot \left[\prod_{t_u=1}^{m} \mu_{A^i_{t_u}}[u(k-t_u)]\right] \cdot \left[\prod_{t_y=1}^{n} \mu_{B^i_{t_y}}[y(k-t_y)]\right]\right\} \cdot \left\{\sum_{i=1}^{l}\left\{\left\{\prod_{t_u=1}^{m} \mu_{A^i_{t_u}}[u(k-t_u)]\right\} \cdot \left\{\prod_{t_y=1}^{n} \mu_{B^i_{t_y}}[y(k-t_y)]\right\}\left[\frac{u(k-t_u)-c^i_{t_u}}{(\sigma^i_{t_u})^2}\right]\right\}\right\}}{\left\{\sum_{i=1}^{l}\left[\left\{\prod_{t_u=1}^{m} \mu_{A^i_{t_u}}[u(k-t_u)]\right\} \cdot \left\{\prod_{t_y=1}^{n} \mu_{B^i_{t_y}}[y(k-t_y)]\right\}\right]\right\}^2} \end{aligned} \tag{11}$$

By changing the variables, Eq. (8) becomes

$$\begin{aligned} \tilde{\mathbf{x}}(k) &= \mathbf{A}(\mathbf{x}_0,\mathbf{u}_0)\tilde{\mathbf{x}}(k-1) + \mathbf{B}(\mathbf{x}_0,\mathbf{u}_0)\tilde{\mathbf{u}}(k-1) \\ \tilde{y}(k) &= \mathbf{c}^T\tilde{\mathbf{x}}(k) \end{aligned} \tag{12}$$

where $\tilde{\mathbf{x}}(k) = \mathbf{x}(k) - \mathbf{x}_0(k)$, $\tilde{\mathbf{u}}(k) = \mathbf{u}(k) - \mathbf{u}_0(k)$, $\tilde{y}(k) = y(k) - y_0(k)$, $\tilde{\mathbf{x}}(0) = 0$.

Since an FBFN is a nonlinear system, the following theorem (Nikolaou and Manousiouthakis, 1989) was used in this work to calculate the dynamic gain:

Let $N:\mathbf{u}\in L_{pe}^{m}\rightarrow\mathbf{y}\in L_{pe}^{n}$ be an unbiased operator and $L_{\mathbf{u}_0}$ be its linearization around the trajectory $\mathbf{u}_0$. Let W be a convex subset of L_p^m. The notations L_p^n and L_{pe}^n are defined as the finite p-norm (Banach) space and the extended Banach space, given by:

$$L_p^n=\{x:[0,\infty)\rightarrow R^n:\|x\|_p<\infty\}\quad L_{pe}^n=\left\{x:[0,\infty)\rightarrow R^n:x_T\in L_p^n\text{ for all }T\geq 0\right\} \tag{13}$$

where the truncated signal x_T is defined as follows:

$$x_T:t\rightarrow x_T(t)=\begin{cases}x(t) & \text{if}\, t\leq T\\ 0 & \text{if}\, t>T\end{cases}, \tag{14}$$

Then, the dynamic gain of N can be calculated from the maximum value of the gains of its linearization L (Nikolaou and Manousiouthakis, 1989):

$$\|N\|_{pW}=\sup_{\substack{\mathbf{u}_1,\mathbf{u}_2\in W\\ \mathbf{u}_1\neq\mathbf{u}_2}}\frac{\|N(\mathbf{u}_1)-N(\mathbf{u}_2)\|_p}{\|\mathbf{u}_1-\mathbf{u}_2\|_p}=\sup_{\mathbf{u}_0\in W}\|L_{\mathbf{u}_0}\|_p,\quad p\in[1,\infty] \tag{15}$$

Based on the obtained models, two methods to estimate the L_2 gain and L_∞ gain of FBFN systems are provided in the next subsections.

2.2. L_2 gain estimation of nonlinear systems represented by FBFN models

It has been proven by Schaft (1992) that, if the local linear model of a nonlinear system has its L_2 gains less than a constant γ, then the local L_2 gain of the nonlinear system will also be less than γ. Since the L_2 gain of a linear system is also its $H\infty$ norm, the L_2 gain of the FBFN can be approximated by finding the maximum of the $H\infty$ norm values of all locally linearized systems:

$$\|N\|_{2W}=\sup_{\mathbf{u}_0\in W}\|L_{\mathbf{u}_0}\|_{H\infty} \tag{16}$$

The local linear systems $L_{\mathbf{u}_o}$ are provided in the form of state space equations as given in Eq. (8). Fast computing techniques such as Bruinsma and Steinbuch (1990) can be used to calculate the values of their H_∞ norm.

2.3. L_∞ gain estimation of nonlinear systems represented by FBFN models

This subsection provides an analytical computation of the L_∞ gain for discrete nonlinear systems and FBFN models. This work is an expansion of Nikolaou and Manousiouthakis' (1987) techniques, which is only applied to continuous nonlinear systems. In Theorem 1, the L_∞ gain of an FBFN is proven to be the solution of a non-smooth optimal control problem, which can be solved numerically by using the non-smooth Newton's method (Gerdts, 2008).

Theorem 1. (Dynamic infinity gain of FBFN systems):

The dynamic infinity gain of a nonlinear system represented by an FBFN model, which is described by Eq. (2), over a convex set $W\triangleq\{\mathbf{u}\in L_\infty:\|\mathbf{u}(k)\|\leq\delta\}$ can be found by solving the following non-smooth optimal control problem:

$$\|N\|_{\Delta\infty W}=\sup_{k\in(0,\infty)}\left[-\inf_{\mathbf{u}_0\in W}\sum_{l=0}^{k-1}-\|\mathbf{c}^T\mathbf{\Phi}(k,l+1)\mathbf{B}\|_i\right] \tag{17}$$

under the dynamic constraints:

$$\begin{aligned}&\mathbf{\Phi}(k+1,l)=\mathbf{A}\mathbf{\Phi}(k,l)\\&\mathbf{\Phi}:(0,\infty)\times[0,\infty)\rightarrow\mathbb{R}^{n\times n},\ \ \mathbf{\Phi}(k,k)=\mathbf{I}\end{aligned} \tag{18}$$

where $\mathbf{A}$ and $\mathbf{B}$ are the coefficient matrices given in Eq. (9). $\|\cdot\|_i$ represents any induced norm.

Proof: For a system represented by Eq. (12), the unique solution can be found as follows (Dahleh and Verghese, 2011):

$$\begin{aligned}&\tilde{\mathbf{x}}(k)=\mathbf{\Phi}(k,0)\tilde{\mathbf{x}}(0)+\sum_{l=0}^{k-1}\mathbf{\Phi}(k,l+1)\mathbf{B}(l)\tilde{\mathbf{u}}(l)\\&\tilde{y}(k)=\mathbf{c}^T\tilde{\mathbf{x}}(k),\end{aligned} \tag{19}$$

where the state transition matrix $\mathbf{\Phi}(k,l)$ relates the state at time k to the state at an earlier time l:

$$\tilde{\mathbf{x}}(k)=\mathbf{\Phi}(k,l)\tilde{\mathbf{x}}(l) \tag{20}$$

and has the following properties:

$$\begin{aligned}&\mathbf{\Phi}(k,k)=\mathbf{I}\\&\tilde{\mathbf{x}}(k)=\mathbf{\Phi}(k,0)\tilde{\mathbf{x}}(0)\\&\mathbf{\Phi}(k+1,l)=\mathbf{A}(k)\mathbf{\Phi}(k,l)\end{aligned} \tag{21}$$

From Eqs. (2) and (19), the output of the system can be calculated from its solution:

$$\tilde{y}(k)=\sum_{l=0}^{k-1}\mathbf{c}^T\mathbf{\Phi}(k,l+1)\mathbf{B}(l)\tilde{\mathbf{u}}(l) \tag{22}$$

Eq. (22) can be rewritten as follows:

$$\tilde{y}(k) = \sum_{l=0}^{k-1} \mathbf{G}_l(k)\tilde{\mathbf{u}}(l) \tag{23}$$

where $\mathbf{G}_l(k) = \mathbf{c}^T\mathbf{\Phi}(k, l+1)\mathbf{B}(l)$. It has been proven by Desoer and Vidyasagar (1975) that, if a time-varying linear system has the responses as provided in Eq. (23), then its L_∞ gain is given as follows:

$$\|L\|_\infty = \sup_{k\in(0,\infty)} \sum_{l=0}^{k-1} \|\mathbf{G}_l(k)\|_i \tag{24}$$

where $\|\mathbf{G}_l(k)\|_i$ is any induced norm of $\mathbf{G}_l(k)$.

By using Eqs. (15) and (24), the infinity gain of the nonlinear system represented by an FBFN model becomes the solution of the following non-smooth optimal control problem:

$$\|N\|_{\infty W} = \sup_{\mathbf{u}_0\in W} \|L_{\mathbf{u}_0}\|_\infty = \sup_{\mathbf{u}_0\in W}\left[\sup_{k\in(0,\infty)} \sum_{l=0}^{k-1} \|\mathbf{c}^T\mathbf{\Phi}(k,l+1)\mathbf{B}(l)\|_i\right] = \sup_{k\in(0,\infty)}\left[-\inf_{\mathbf{u}_0\in W} \sum_{l=0}^{k-1} -\|\mathbf{c}^T\mathbf{\Phi}(k,l+1)\mathbf{B}(l)\|_i\right] \tag{25}$$

3. Design a stable MLFC with an adaptive output scaling factor

In this section, the novel MLFC with an adaptive output scaling factor (AMLFC) is proposed with three layers. The first layer acts as a conventional fuzzy controller while the second and third layers are used to tune the output scaling factor of the first layer.

Fig. 1 describes an implementation of a nonlinear fuzzy control system. The summation symbol represents the integration operation, which effectively makes the controller a PI-type fuzzy controller. The plant is a general nonlinear dynamic system as in the form of Eq. (2). The control effort $u(k)$ that drives the plant can be computed as follows:

$$\begin{aligned}\bar{u}(k) &= \bar{u}(k-1) + T\Delta u(k)\\ u(k) &= K_{out}\bar{u}(k)\end{aligned} \tag{26}$$

where $\Delta u(k)$ is the output of the first layer and K_{out} is the output scaling factor, which can be adjusted by the second and third layers.

As shown in Fig. 2, the first layer fuzzy mechanism uses two input signals, which are the error $e(k)$ and the time rate of change of error $r(k)$:

$$e(k) = y_{ref}(k) - y(k), \quad r(k) = \frac{e(k)-e(k-1)}{T} \tag{27}$$

where $y_{ref}(k)$ is the referenced signal, T is the sampling time, and k is the sampling instance. The scaling factors K_e and K_r of the input signals are adopted to normalize the values of $e(k)$ and $r(k)$:

$$\bar{e}(k) = K_e e(k), \quad \bar{r}(k) = K_r r(k) \tag{28}$$

Each input of the first layer has $2n+1$ membership-functions. The membership functions of the error and the time rate of change of the error are denoted by E_i and R_j (Fig. 3), while the membership functions of the output are denoted by U_j (Fig. 4), with $i = -n, -n+1, \ldots, n-1, n$ and $j = -m, -m+1, \ldots, m-1, m$. Since the inputs are normalized into the range $[-1, 1]$, the distance L between two adjacent membership functions is $1/n$.

The fuzzy rules to calculate the controller output $\Delta u(k)$ are presented in linguistic form as follows:

$$\text{Rule } (i,j): \ \textit{IF } \bar{e} \text{ is } \mathrm{E}_i \text{ AND } \bar{r} \text{ is } \mathrm{R}_j \text{ THEN } \Delta u \text{ is } U_{i,j} \tag{29}$$

where $U_{i,j}$ is the output membership function corresponding to the input membership functions E_i and R_j. The rule base of the first layer (Table 1) is similar to the conventional PI fuzzy controller and can be regarded as a human expert who makes the decision for control effort based on the input signals. In Table 1 (Xu and Shin, 2005), the entries near the center position, where the output signal is near the set point, always have smaller values. A small control effort provides a fast convergence rate and reduces the overshoot when the signal is near the set points. As the signal moves away from the set point, the control effort increases in order to reduce the transient time. It should also be noted that the rule-base table is symmetric about the set point.

The second layer (Fig. 2) uses the error and the time rate of change of the error signals to adjust the output scaling factor of the first layer to reduce the rise time and suppress the oscillation of the system output. In this layer, the change in output scaling factor $\Delta K_\alpha(k)$ is computed by using the following fuzzy rules:

$$\text{Rule } (i,j): \text{If } \bar{e} \text{ is } E_i \text{ and } \bar{r} \text{ is } R_j \text{ then } \Delta K_\alpha(k) \text{ is } D_\alpha \tag{30}$$

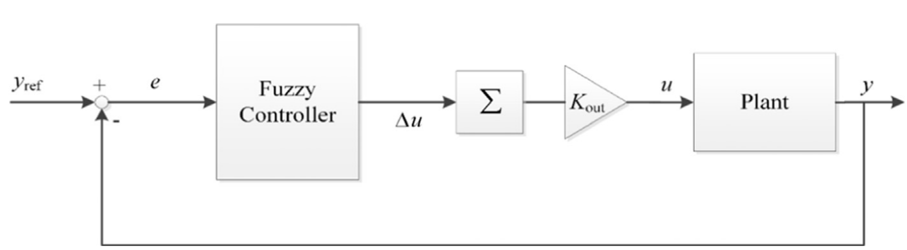

Fig. 1. The closed-loop fuzzy control system.

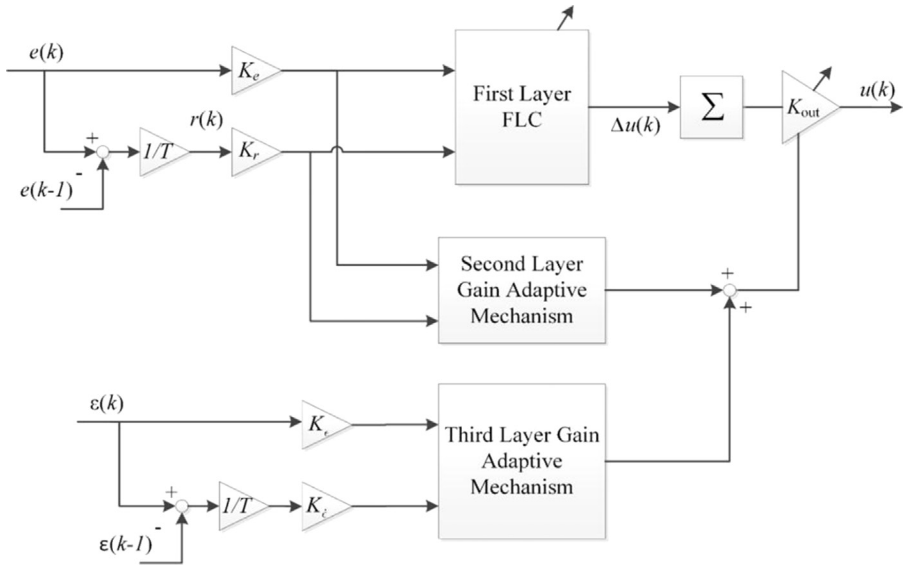

Fig. 2. AMLFC controller.

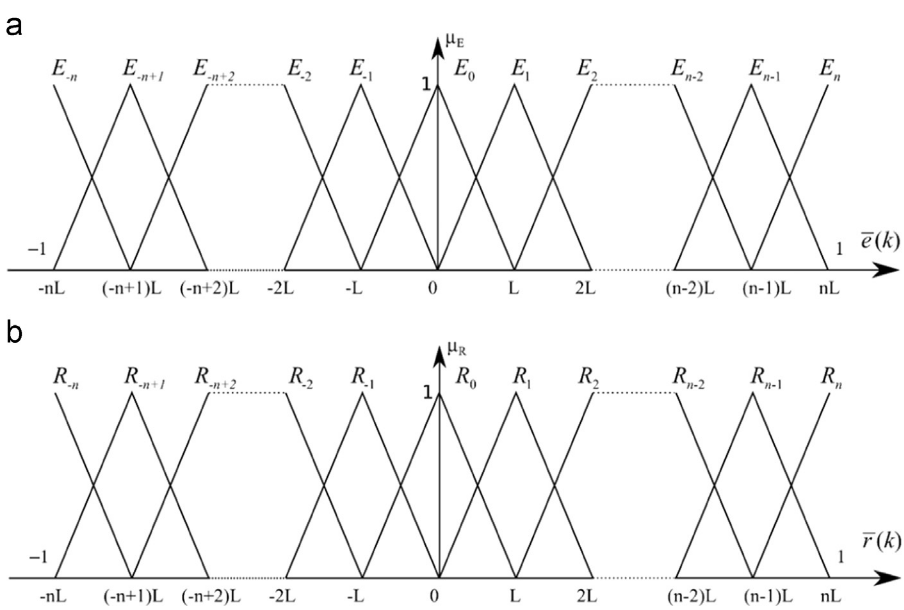

Fig. 3. Input membership functions (a) Error, (b) Time rate of change of error.

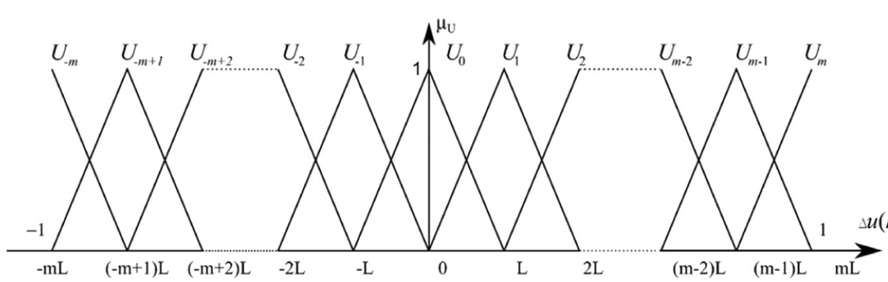

Fig. 4. Output membership functions.

where D_α is the linguistic value of $\Delta K_\alpha(k)$. The rule base for the second layer (Table 2) was developed based on the fuzzy rule base designed by Mudi and Pal (1999). However, while Mudi and Pal's objective was to determine the value of the scaling factor based on the error and the time rate of change of the error signal, the rule base in this paper is designed for the calculation of the necessary change in the output scaling factor. As shown in Table 2, if there is a large error in the output signal while the output is moving away from the reference signal ($\overline{e} \to 1,\ \overline{r} \to 1$ or $\overline{e} \to -1,\ \overline{r} \to -1$), the scaling factor is increased ($D_\alpha \to 0.5$) so that the rise and settling time can be reduced. When the system output is moving into the reference signal ($\overline{e}\cdot\overline{r}<0$) or the error and the time rate of change of the error are very small ($\overline{e}\rightarrow 0,\ \overline{r}\rightarrow 0$), the scaling factor is reduced ($D_\alpha \rightarrow -0.5$) to suppress the amount of overshoot. This rule base is not unique and modifications may be made in accordance with desired system responses.

In order to achieve the desired system performances such as rise time, settling time, and percent overshoot, the designer can specify a reference model for the adaptation process. The objective of the third layer is to make the output of the closed-loop system approach that of the reference model. This layer uses the performance error ϵ and the time rate of change of the performance error $\dot{\epsilon}$ between the output of the control system and the reference model to tune the output scaling factor:

$$\epsilon(k)=y_d(k)-y(k),\quad \dot{\epsilon}(k)=\frac{\epsilon(k)-\epsilon(k-1)}{T} \tag{31}$$

where y_d is the desired output of the reference model. The performance error and the time rate of change of performance error signals have membership functions similar to those of the output error and the time rate of change of the error (Fig. 3).

Since the output error $e(k)$ and the time rate of change of the error signal $r(k)$ always exist whenever there is a change in command signals, the performance errors $\epsilon(k)$ and $\dot{\epsilon}(k)$ are used instead of the output error signals. This way, the adaptation by the third layer can be minimized when the system output has approached the reference model output. The rule base of the first layer (Table 1) is applied in the third layer since they have similar functional objectives. Similarly to the first layer, the Mamdani fuzzy inference mechanism is also applied in the third layer to compute the output scaling factor updating value $\Delta K_\beta(k)$ by the following fuzzy rules:

$$\text{Rule } (i,j): \text{If } \overline{\epsilon} \text{ is } E_i \text{ and } \overline{\dot{\epsilon}} \text{ is } R_j \text{ then } \Delta K_\beta(k) \text{ is } D_\beta \tag{32}$$

where D_β is the linguistic value of $\Delta K_\beta(k)$, $\overline{\epsilon}$ and $\overline{\dot{\epsilon}}$ are the normalized values of the performance error, and the time rate of change of the performance error by the same scaling factors as $e(k)$ and $r(k)$:

$$\overline{\epsilon}(k)=K_e\epsilon(k),\quad \overline{\dot{\epsilon}}(k)=K_r\dot{\epsilon}(k) \tag{33}$$

With the addition of the second and third layers, the output scaling factor of the first layer can be calculated by using the following formula:

$$K_{out}(k)=\min\left(K_{out}(k-1)+\alpha\Delta K_\alpha(k)+\beta\Delta K_\beta(k), K_{\max}\right) \tag{34}$$

Table 1
Rule base of the first and third layer fuzzy controllers.

		Time rate of change of the error										
		−1.0	−0.8	−0.6	−0.4	−0.2	0.0	0.2	0.4	0.6	0.8	1.0
	−1.0	1.00	1.00	1.00	1.00	1.00	1.00	0.80	0.60	0.30	0.10	0.00
	−0.8	1.00	1.00	1.00	1.00	1.00	0.80	0.60	0.30	0.10	0.00	−0.10
	−0.6	1.00	1.00	1.00	1.00	0.80	0.60	0.30	0.10	0.00	−0.10	−0.30
	−0.4	1.00	1.00	1.00	0.80	0.60	0.30	0.10	0.00	−0.10	−0.30	−0.60
	−0.2	1.00	1.00	0.80	0.60	0.30	0.11	0.00	−0.10	−0.30	−0.60	−0.80
Error	0.0	1.00	0.80	0.60	0.30	0.10	0.00	−0.10	−0.30	−0.60	−0.80	−1.00
	0.2	0.80	0.60	0.30	0.10	0.00	−0.10	−0.31	−0.60	−0.80	−1.00	−1.00
	0.4	0.60	0.30	0.10	0.00	−0.10	−0.30	−0.60	−0.80	−1.00	−1.00	−1.00
	0.6	0.30	0.10	0.00	−0.10	−0.30	−0.60	−0.80	−1.00	−1.00	−1.00	−1.00
	0.8	0.10	0.00	−0.10	−0.30	−0.60	−0.80	−1.00	−1.00	−1.00	−1.00	−1.00
	1.0	0.00	−0.10	−0.30	−0.60	−0.80	−1.00	−1.00	−1.00	−1.00	−1.00	−1.00

Table 2
Fuzzy rule base for computation of D_α (second layer).

		Time rate of change of the error						
		−1	−0.7	−0.3	0	0.3	0.7	1
	−1	0.5	0.5	0.5	0.3	0.1	−0.1	−0.3
	−0.8	0.5	0.5	0.3	0.1	−0.1	−0.3	−0.5
	−0.6	0.5	0.3	0.1	−0.1	−0.3	−0.5	−0.5
	−0.4	0.3	0.1	−0.1	−0.3	−0.5	−0.5	−0.5
	−0.2	0.1	−0.1	−0.3	−0.4	−0.5	−0.5	−0.5
Error	0	−0.5	−0.5	−0.5	−0.5	−0.5	−0.5	−0.5
	0.2	−0.5	−0.5	−0.5	−0.4	−0.3	−0.1	0.1
	0.4	−0.5	−0.5	−0.5	−0.3	−0.1	0.1	0.3
	0.6	−0.5	−0.5	−0.3	−0.1	0.1	0.3	0.5
	0.8	−0.5	−0.5	−0.1	0.1	0.3	0.5	0.5
	1	−0.3	−0.1	0.1	0.3	0.5	0.5	0.5

where α and β are the adaptation rates of the second layer and the third layer, respectively. The minimum function in Eq. (34) ensures that the output scaling factorK_{out} does not exceed the maximum value $K_{\max}$ at which the control system remains stable:

$$K_{\max} = \frac{L}{2(K_e T + K_r)\|N\|_{pW}} \tag{35}$$

where $\|N\|_{pW}$ is the p-gain of the nonlinear plant as defined in Eq. (15). The derivation of $K_{\max}$ and the stability analysis of the fuzzy control systems are presented in the next section.

4. Stability condition for FBFN-based PI fuzzy control systems

By utilizing the small gain theorem, an approach similar to that proposed by Chen and Ying (1993) is used in the current work to obtain the stability condition for the fuzzy control systems. However, the stability problem in Chen and Ying (1993) was divided by the locations of the error and the time rate of change of the error with respect to zero. Hence, the upper bounds of the fuzzy controller have different values whenever the error or the time rate of change of the error moves from one membership function to the other. The stability analysis cannot be easily extended since the complexity of the problem will grow significantly when the numbers of input and output membership functions are increased. Therefore, only fuzzy controllers with two input and three output membership functions were analyzed by Chen and Ying (1993). In this work, the stability problem is divided by the locations of the error and the time rate of change of the error with respect to the activated membership functions, as shown in Fig. 5 and Table 3. Since the upper bounds of the fuzzy controller have been found to have similar values in each location, the results can be generalized for fuzzy controllers with large numbers of input and output membership functions.

The conditions of the error and the time rate of change of error relative to the activated membership functions for case 1 (Fig. 6) are given by:

$$L\left(p+\frac{1}{2}\right) < \bar{e} < L(p+1) \text{ AND } L\left(q+\frac{1}{2}\right) < \bar{r} < L(q+1) \text{ AND } \bar{e} - L\left(p+\frac{1}{2}\right) < \bar{r} - L\left(q+\frac{1}{2}\right) \tag{36}$$

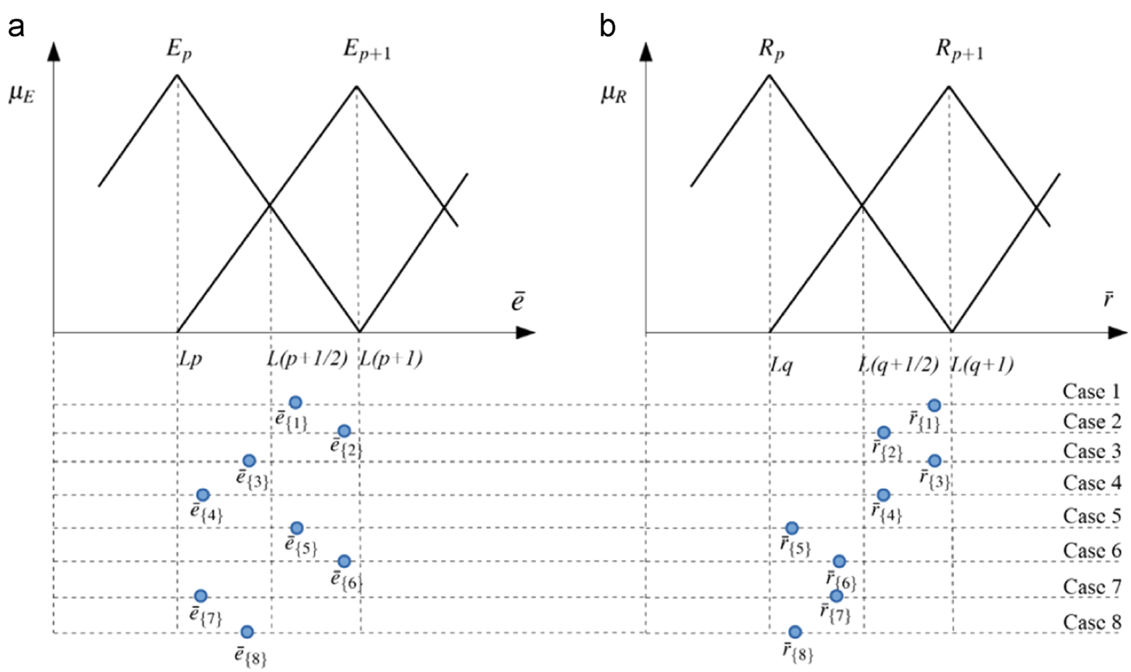

Fig. 5. Locations of the error and the time rate of change of the error in relation to the activated membership functions.

Table 3
Conditions of error and rate of change in error.

Case	Conditions of the error and the time rate of change of the error
1	$L(p+\frac{1}{2}) < \bar{e} < L(p+1)$ AND $L(q+\frac{1}{2}) < \bar{r} < L(q+1)$ AND $\bar{e} - L(p+\frac{1}{2}) < \bar{r} - L(q+\frac{1}{2})$
2	$L(p+\frac{1}{2}) < \bar{e} < L(p+1)$ AND $L(q+\frac{1}{2}) < \bar{r} < L(p+1)$ AND $\bar{e} - L(p+\frac{1}{2}) > \bar{r} - L(q+\frac{1}{2})$
3	$Lp < \bar{e} < L(p+\frac{1}{2})$AND $L(q+\frac{1}{2}) < \bar{r} < L(q+1)$ AND $L(p+\frac{1}{2}) - \bar{e} < \bar{r} - L(q+\frac{1}{2})$
4	$Lp < \bar{e} < L(p+\frac{1}{2})$AND $L(q+\frac{1}{2}) < \bar{r} < L(q+1)$ AND $L(p+\frac{1}{2}) - \bar{e} > \bar{r} - L(q+\frac{1}{2})$
5	$L(p+\frac{1}{2}) < \bar{e} < L(p+1)$ AND $Lq < \bar{r} < L(q+\frac{1}{2})$ AND $\bar{e} - L(p+\frac{1}{2}) < L(q+\frac{1}{2}) - \bar{r}$
6	$L(p+\frac{1}{2}) < \bar{e} < L(p+1)$ AND $Lq < \bar{r} < L(q+\frac{1}{2})$ AND $\bar{e} - L(p+\frac{1}{2}) > L(q+\frac{1}{2}) - \bar{r}$
7	$Lp < \bar{e} < L(p+\frac{1}{2})$ AND $Lq < \bar{r} < L(q+\frac{1}{2})$ AND $\bar{e} - Lp < \bar{r} - Lq$
8	$Lp < \bar{e} < L(p+\frac{1}{2})$ AND $Lq < \bar{r} < L(q+\frac{1}{2})$ AND $\bar{e} - Lp > \bar{r} - Lq$

By assuming that E_p, E_{p+1}, R_q, and R_{q+1} are four non-zero input membership functions of the error and the time rate of change of the error, the membership values can be found as follows:

$$\mu_{E_{(p)}} = \frac{L(p+1)-K_e e}{L}, \quad \mu_{E_{(p+1)}} = \frac{K_e e - Lp}{L} \tag{37}$$

$$\mu_{R_{(q)}} = \frac{L(q+1)-K_r r}{L}, \quad \mu_{R_{(q+1)}} = \frac{K_r r - Lq}{L} \tag{38}$$

The premises $H_{i,j}$ $(i=p,p+1$ and $j=q,q+1)$ of the four activated rules for case 1 are calculated by using the minimum operations:

$$H_{p,q} = \min\left(\mu_{E_p}(e), \mu_{R_q}(r)\right) = \mu_{R_q}(r) = \frac{L(q+1)-K_r r}{L} \tag{39}$$

$$H_{p+1,q} = \min\left(\mu_{E_{p+1}}(e), \mu_{R_q}(r)\right) = \mu_{R_q}(r) = \frac{L(q+1)-K_r r}{L} \tag{40}$$

$$H_{p,q+1} = \min\left(\mu_{E_p}(e), \mu_{R_{q+1}}(r)\right) = \mu_{E_p}(e) = \frac{L(p+1)-K_e e}{L} \tag{41}$$

$$H_{p+1,q+1} = \min\left(\mu_{E_{p+1}}(e), \mu_{R_{q+1}}(r)\right) = \mu_{E_{p+1}}(e) = \frac{K_e e - Lp}{L} \tag{42}$$

The change in control output $\Delta u(k)$ can be calculated by using singleton fuzzification, minimum inference, and centroid defuzzification methods:

$$\begin{aligned}
\Delta u(k) &= \frac{\sum_{i,j} U_{i,j} \cdot \min\left[\mu_{E_i}(\bar{e}), \mu_{E_j}(\bar{r})\right]}{\sum_{i,j} \min\left[\mu_{E_i}(\bar{e}), \mu_{E_j}(r)\right]} = \frac{\sum_{i,j} U_{i,j} \cdot H_{i,j}}{\sum_{i,j} H_{i,j}}, \quad (i=p,p+1 \text{ and } j=q,q+1) \\
&= \frac{\frac{U_{p,q}L(q+1)-K_r r}{L} + \frac{U_{p+1,q}L(q+1)-K_r r}{L} + \frac{U_{p,q+1}L(p+1)-K_e e}{L} + \frac{U_{p+1,q+1}K_e e - Lp}{L}}{\frac{L(q+1)-K_r r}{L} + \frac{L(q+1)-K_r r}{L} + \frac{L(p+1)-K_e e}{L} + \frac{K_e e - Lp}{L}} \\
&= \frac{-U_{p,q+1}+U_{p+1,q+1}K_e e + -U_{p,q} - U_{p+1,q}K_r r + qLU_{p,q} + U_{p+1,q} + pLU_{p,q+1} - U_{p+1,q+1} + LU_{p,q} + U_{p+1,q} + U_{p,q+1}}{2qL+3L-2K_r r}
\end{aligned} \tag{43}$$

By repeating the same procedure for all other cases, the change in control output $\Delta u(k)$ can be formulated into the following form:

$$\Delta u(k) = \frac{G_e K_e e + G_r K_r r + C}{D} \tag{44}$$

where the parameters G_e, G_r, C and D are given in Tables 4 and 5.

From here, the stability condition for nonlinear PI fuzzy control systems can be stated as follows:

Theorem 2. The sufficient conditions for the nonlinear PI fuzzy control system shown in Fig. 1 to be input-and-output stable are as follows:

1. The nonlinear process has a finite p-gain: $\|N\|_{pW} < \infty$
2. The maximum output scaling factor of the PI fuzzy controller satisfies the following condition:

$$K_{out} \le K_{\max} = \frac{L}{2K_e T + K_r \|N\|_{pW}} \tag{45}$$

Proof: First, a closed-loop system is constructed in such a way that it is mathematically equivalent to the fuzzy control system shown in Fig. 1. The equivalent system includes two nonlinear processes connected in a feedback loop (Fig. 7), S_1 and S_2, which are defined as follows:

$$\begin{aligned}
S_1(e_1(k)) &= T\Delta u(k) = T\frac{\left(G_e K_e + \frac{G_r K_r}{T}\right)e(k) - \frac{G_r K_r}{T}e(k-1) + C}{2qL+3L-2K_r r} \\
S_2(e_2(k)) &= N(u(k)) = N(K_{out} e_2(k))
\end{aligned} \tag{46}$$

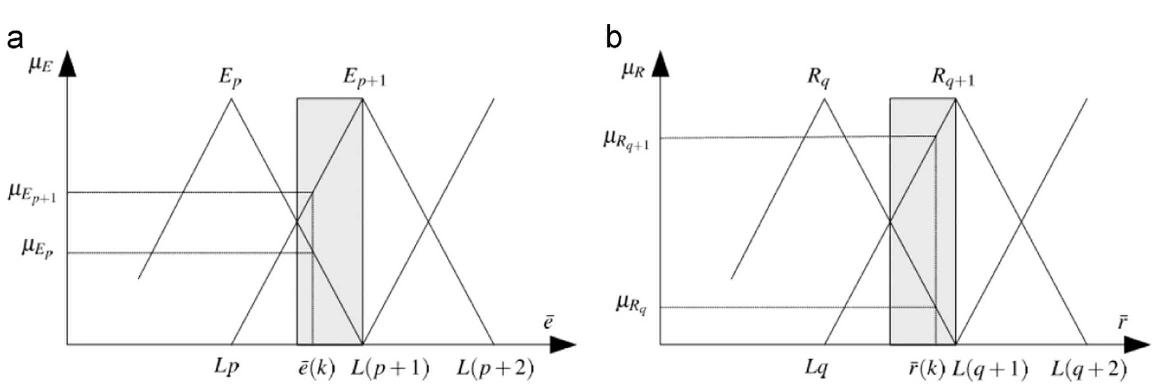

Fig. 6. Locations of the error and the time rate of change of the error in Case 1.

Table 4
Values of G_e, G_r, and D.

Case	G_e	G_r	D
1	$-U_{p,q+1}+U_{p+1,q+1}$	$-U_{p,q}-U_{p+1,q}$	$2qL+3L-2K_r r$
2	$-U_{p,q}-U_{p,q+1}$	$-U_{p+1,q}+U_{p+1,q+1}$	$2Lp+3L-2K_e e$
3	$-U_{p,q+1}+U_{p+1,q+1}$	$-U_{p,q}-U_{p+1,q}$	$2qL+3L-2K_r r$
4	$U_{p+1,q}+U_{p+1,q+1}$	$-U_{p,q}+U_{p,q+1}$	$2K_e e+L-2Lp$
5	$-U_{p,q}+U_{p+1,q}$	$U_{p,q+1}+U_{p+1,q+1}$	$2K_r r-2qL+L$
6	$-U_{p,q}-U_{p,q+1}$	$-U_{p+1,q}+U_{p+1,q+1}$	$2Lp+3L-2K_e e$
7	$U_{p+1,q}+U_{p+1,q+1}$	$-U_{p,q}+U_{p,q+1}$	$2K_e e+L-2Lp$
8	$-U_{p,q}+U_{p+1,q}$	$U_{p,q+1}+U_{p+1,q+1}$	$2K_r r-2qL+L$

Table 5
Values of C.

Case	C
1	$qL(U_{p,q}+U_{p+1,q})+pL(U_{p,q+1}-U_{p+1,q+1})+L(U_{p,q}+U_{p+1,q}+U_{p,q+1})$
2	$qL(U_{p+1,q}-U_{p+1,q+1})+pL(U_{p,q}+U_{p,q+1})+L(U_{p,q}+U_{p+1,q}+U_{p,q+1})$
3	$qL(U_{p,q}+U_{p+1,q})+pL(U_{p,q+1}-U_{p+1,q+1})+L(U_{p,q}+U_{p+1,q}+U_{p,q+1})$
4	$qL(U_{p,q}-U_{p,q+1})+pL(-U_{p+1,q}-U_{p+1,q+1})+LU_{p,q}$
5	$qL(-U_{p,q+1}-U_{p+1,q+1})+pL(U_{p,q}-U_{p+1,q})+LU_{p,q}$
6	$qL(U_{p+1,q}-U_{p+1,q+1})+pL(U_{p,q}-U_{p,q+1})+L(U_{p,q}+U_{p+1,q}+U_{p,q+1})$
7	$qL(U_{p,q}-U_{p,q+1})+pL(U_{p+1,q}-U_{p+1,q+1})+LU_{p,q}$
8	$qL(-U_{p,q+1}-U_{p+1,q+1})+pL(U_{p,q}-U_{p+1,q})+LU_{p,q}$

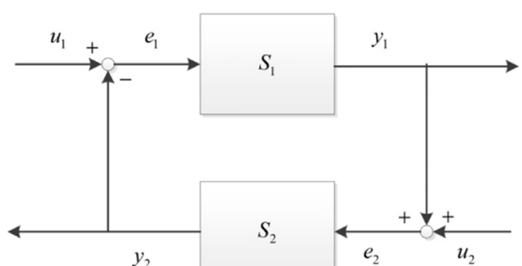

Fig. 7. An equivalent closed-loop control system.

where $N(u(k))$ is the nonlinear operator that represents the plant. The inputs of the equivalent closed-loop system are u_1 and u_2:

$$u_1(k)=y_{ref}(k), \quad u_2(k)=\frac{\overline{u}(k-1)}{K_{out}} \tag{47}$$

From the schematic diagram in Fig. 7, the values of $e_1(k)$ and $e_2(k)$ can be found as follows:

$$e_1(k)=u_1(k)-S_2(e_2(k))=y_d(k)-N(u(k))=e(k) \tag{48}$$

$$e_2(k)=S_1(e_1(k))+u_2(k)=T\Delta u(k)+\frac{\overline{u}(k-1)}{K_{out}}=\frac{u(k)}{K_{out}}=\overline{u}(k) \tag{49}$$

In Case 1, since $K_r r<L(q+1)$, the following inequalities can be obtained:

$$D=2qL+3L-2K_r r>L>0 \tag{50}$$

and

$$\left(G_eK_e+\frac{G_rK_r}{T}\right)e(k)-\frac{G_rK_r}{T}e(k-1)+C\le\left|G_eK_e+\frac{G_rK_r}{T}\right||e_1(k)|+\left|-\frac{G_rK_r}{T}e(k-1)+C\right|$$
$$\le\frac{T|G_eK_e|+|G_rK_r|}{T}|e_1(k)|+\frac{T|C|+|G_rK_r||e(k-1)|}{T} \tag{51}$$

As the output membership functions $U_{i,j}$ are bounded by $[-1,1]$, the following were used:

$$|-U_{p,q+1}+U_{p+1,q+1}|\le|U_{p,q+1}|+|U_{p+1,q+1}|\le 2$$
$$|U_{p,q}-U_{p+1,q}|\le|U_{p,q}|+|U_{p+1,q}|\le 2 \tag{52}$$

From the definition of $S_1(e_1(k))$ in Eq. (46), the values of G_e and G_r for case 1 in Table 4, and the inequalities in Eq. (50), (51), and (52), the upper bound of $S_1(e_1(k))$ can be computed as follows:

$$S_1(e_1(k))=T\frac{(G_eK_e+\frac{G_rK_r}{T})e(k)-\frac{G_rK_r}{T}e(k-1)+C}{2qL+3L-2K_r r}\le\frac{T|G_eK_e|+|G_rK_r|}{L}|e_1(k)|+\frac{T|C|+|G_rK_r||e(k-1)|}{L}$$

$$= \frac{TK_e\left|-U_{p,q+1}+U_{p+1,q+1}\right|+K_r\left|U_{p,q}-U_{p+1,q}\right|}{L}\left|e_1(k)\right| + \frac{T|C|+|G_rK_r|M_e}{L}$$
$$\le \frac{2(K_eT+K_r)}{L}\left|e_1(k)\right| + \frac{T|C|+|G_rK_r|M_e}{L} = \gamma_1\left|e_1(k)\right| + \beta_1 \tag{53}$$

where M_e is the maximum magnitude of the error signal $M_e = \sup_{k \ge 0}|e(k)|$, and

$$\gamma_1 = \frac{2(K_eT+K_r)}{L}, \quad \beta_1 = \frac{T|C|+|G_rK_r|M_e}{L} \tag{54}$$

Similarly, the upper bound of $S_2(e_2(k))$ can be obtained by using the properties of norm operations as follows:

$$S_2(e_2(k)) = N(K_{out}e_2(k)) \le K_{out}\|N\|_{pW}\left|e_2(k)\right| = \gamma_2\left|e_2(k)\right| \tag{55}$$

where $\|N\|_{pW}$ is the gain of the nonlinear operator $N(\cdot)$ defined in Eq. (15) and $\gamma_2 = K_{out}\|N\|_{pW}$.

From Eq. (54) and the fact that the operator S_1 can be considered as a time-varying linear system, the gain of the operator S_1 becomes:

$$\|S_1\|_{pW} = \gamma_1, \tag{56}$$

which is a finite number. By applying the small gain theorem to the feedback system in Fig. 7, the requirements for the fuzzy closed-loop system to be stable input-output are obtained as follows:

$$\gamma_2 = K_{out}\|N\|_{pW} < \infty \text{ and } \gamma_1\gamma_2 < 1 \tag{57}$$

Because $K_{out} < \infty$, by substituting γ_1 and γ_2 found above into Eq. (57), the stability requirements become:

$$\|N\|_{pW} < \infty \quad \text{and} \quad \frac{2(K_eT+K_r)}{L}K_{out}\|N\|_{pW} < 1 \tag{58}$$

Repeating the same procedure will also yield the same results for the remaining cases. Therefore, the maximum output scaling factor of the fuzzy controller is as follows:

$$K_{\max} = \frac{L}{2K_eT + K_r\|N\|_{pW}} \tag{59}$$

Theorem 2**.** provides a systematic stability condition for controlling nonlinear systems by using PI fuzzy controllers. The proposed stability condition is a simple design practice since it only requires the output scaling-factor of a PI fuzzy controller to be bounded. For future works, the stability theory can be extended into PID fuzzy control systems by utilizing the structural analysis of the PID controller proposed by Haj-Ali and Ying (2004, 2003).

5. Simulation Results

Performance comparisons between the AMLFC and the robust adaptive fuzzy controller (RAFC) proposed by Wu et al. (2013) are presented in this section. MATLAB/SIMULINK simulations were conducted on a three-dimensional tower crane system (Wu et al., 2013).

The control variables of the tower crane system are the tower motor voltage M_θ (V) and the trolley motor voltage $M_F(V)$:

$$u_1 = M_\theta, \quad u_2 = M_F \tag{60}$$

Four outputs of the system are the distance between the trolley and the tower x_p, the slew angle of the tower θ_γ, the deflection angles α and β of the payload in the Y-Z, and the X-Z plane.

By using $x_{11} = x_p$, $x_{12} = \dot{x}_p$, $x_{21} = \beta$, $x_{22} = \dot{\beta}$, $x_{31} = \theta_r$, $x_{32} = \dot{\theta}_r$, $x_{41} = \alpha$, $x_{42} = \dot{\alpha}$ as the state variables, the equations of motion of the tower crane system are given by (Wu et al., 2013):

$$\dot{x}_{12} = K_{mx}u_1 - m_tgx_{21} + h_1(t)x_{11}(t-\tau_1) + d_1$$
$$\dot{x}_{22} = \frac{K_{mx}}{L}u_1 - \frac{m_tg}{L}x_{21} - \frac{g}{L}x_{21} - \frac{K_{mr}x_{41}u_2}{1+M_rx_{11}^2} - \frac{m_rgx_{11}x_{41}^2}{1+M_rx_{11}^2} + h_2(t)x_{21}(t-\tau_2) + d_2$$
$$\dot{x}_{32} = \frac{K_{mr}u_2 + m_rgx_{11}x_{41}}{1+M_rx_{11}^2} + h_3(t)x_{31}(t-\tau_3) + d_3$$
$$\dot{x}_{42} = \frac{(K_{mr}u_2 + m_rgx_{11}x_{41})x_{21}}{1+M_rx_{11}^2} - \frac{gx_{41}}{L} - \frac{(K_{mr}u_2 + m_rgx_{11}x_{41})x_{11}}{1+M_rx_{11}^2} + h_4(t)x_{41}(t-\tau_4) + d_4 \tag{61}$$

Table 6
Parameters of the tower crane system (Wu et al., 2013).

Parameter	Notation	Value
Payload length	L	0.1 m
Mass of trolley	M	0.465 kg
Mass of payload	m	0.125 kg
Payload mass relative to J_0	m_r	0.142 kg
Trolley mass relative to J_0	M_r	0.53 kg
Motor equivalent moment of inertia	J_0	0.877 $kg\,m^2$
Acceleration gain for trolley servo	K_{mx}	0.9 m/s^2
Acceleration gain for tower servo	K_{mr}	3.33 rad/s^2V

where $\tau_1 = 0.2s$, $\tau_2 = 0.1s$, $\tau_3 = 0.15s$, $\tau_4 = 0.1s$ are time-delay constants, $m_t = m/M$, $h_q(t)$, $q = 1...4$ are time-varying functions:

$$h_1 = h_3 = 0.01\ \sin(t), \quad h_2 = h_4 = 0.01\ \cos(t) \tag{62}$$

The disturbances d_1, d_2, d_3, and d_4 are functions of time:

$$d_1 = d_3 = 0.1\ \sin(t)\exp(-0.2t), \quad d_2 = d_4 = 0.1\ \cos(t)\exp(-0.2t) \tag{63}$$

Other system parameters can be found in Table 6.

With the following simple feedback gains to stabilize the plant:

$$\mathbf{K} = [k_{11} \quad k_{12} \quad k_{21} \quad k_{22} \quad k_{31} \quad k_{32} \quad k_{41} \quad k_{42}] = [1 \quad 1 \quad 0 \quad 0 \quad 1 \quad 1 \quad -10 \quad -10], \tag{64}$$

the equations of the system then become:

$$\begin{aligned}
\dot{x}_{12} &= K_{mx}(\zeta_1 - k_1 x_{11} - k_2 x_{12}) - m_t g x_{21} + h_1(t) x_{11}(t-\tau_1) + d_1 \\
\dot{x}_{22} &= \frac{K_{mx}}{L}(\zeta_1 - k_1 x_{11} - k_2 x_{12}) - \frac{m_t g}{L} x_{21} - \frac{g}{L} x_{21} - \frac{K_{mr} x_{41}(\zeta_2 - k_{31}x_{31} - k_{32}x_{32} - k_{41}x_{41} - k_{42}x_{42})}{1 + M_r x_{11}^2} \\
&\quad - \frac{m_r g x_{11} x_{41}^2}{1 + M_r x_{11}^2} + h_2(t) x_{21}(t-\tau_2) + d_2 \\
\dot{x}_{32} &= \frac{K_{mr}(\zeta_2 - k_{31}x_{31} - k_{32}x_{32} - k_{41}x_{41} - k_{42}x_{42}) + m_r g x_{11} x_{41}}{1 + M_r x_{11}^2} + h_3(t) x_{31}(t-\tau_3) + d_3 \\
\dot{x}_{42} &= \frac{[K_{mr}(\zeta_2 - k_{31}x_{31} - k_{32}x_{32} - k_{41}x_{41} - k_{42}x_{42}) + m_r g x_{11} x_{41}] x_{21}}{1 + M_r x_{11}^2} - \frac{g x_{41}}{L} - \frac{(K_{mr} u_2 + m_r g x_{11} x_{41}) x_{11}}{1 + M_r x_{11}^2} \\
&\quad + h_4(t) x_{41}(t-\tau_4) + d_4
\end{aligned} \tag{65}$$

where ζ_1 and ζ_2 are new system inputs. Since the inputs and outputs of the system are uncoupled, the feedback system can be divided into two independent subsystems: $y_1 = N_1(\gamma_1)$ and $y_2 = N_2(\gamma_2)$.

By using least square methods and genetic algorithms (Lee and Shin, 2003), the training of the FBFNs was conducted on MATLAB. Fig. 8 shows the non-dimensional error indices (NDEI) during the training process. Two FBFN models with 61 and 26 hidden nodes were obtained to approximate the first and the second process, respectively:

$$\begin{array}{ll}
\text{Rule i } (u_1 - y_1): & \text{Rule i } (u_2 - y_2): \\
\text{If} u_1(k-1) = A_{11}^i, ..., \ u_1(k-6) = A_{16}^i & \text{If} u_2(k-1) = A_{21}^i, \ \ldots, \ u_1(k-3) = A_{23}^i \\
y_1(k-1) = B_{11}^i, \ ..., \ y_1(k-6) = B_{16}^i, & y_2(k-1) = B_{21}^i, \ \ldots, \ y_2(k-3) = B_{23}^i, \\
\text{then } y_1(k) = b_1^i & \text{then } y_2(k) = b_2^i
\end{array}$$

From the obtained FBFNs, linearized models of the systems at different operating conditions were calculated by Eq. (9). Their H∞ norms can then be found by using the non-smooth Newton's method (Gerdts, 2008) and are given in Fig. 9 for all the training data sets.

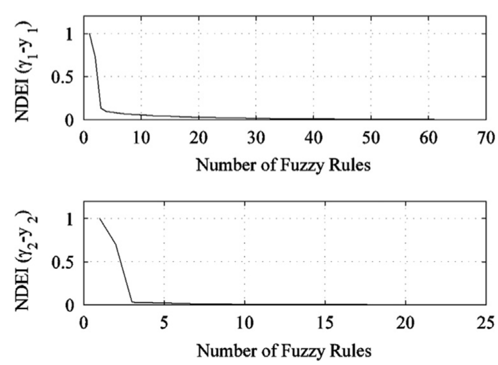

Fig. 8. NDEI during FBFN training of the tower crane system.

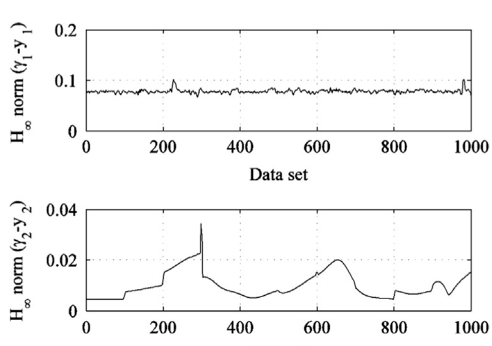

Fig. 9. H∞ norm of the tower crane's local systems.

The L_2-gains of the FBFNs were estimated by taking the maximum values of the linearized models' H∞ norms:

$$\|N_1\|_{2W} = 0.1, \quad \|N_2\|_{2W} = 0.04 \tag{66}$$

where $\|N_1\|_{2W}$ and $\|N_2\|_{2W}$ denote the L_2-gains of the first process $(\gamma_1 - y_1)$, and the second process $(\gamma_2 - y_2)$ respectively; W represents the input space $W \triangleq \{u \in \mathbb{R}\}$.

The reference signals for the trolley translational position and the jib angular position are 0.06 m, respectively. Two AMLFCs were used to control the two subsystems. The scaling factors for three layers of each fuzzy controller were selected as follows:

$$K_{e1} = 6,\ K_{r1} = 0.1,\ K_{\epsilon1} = 30,\ K_{\dot{\epsilon}1} = 30,\ K_{out1(\text{initial})} = 3,\ \alpha_1 = 0.01,\ \beta_1 = 2 \tag{67}$$

$$K_{e2} = 1,\ K_{r2} = 0.1,\ K_{\epsilon2} = 0.1,\ K_{\dot{\epsilon}2} = 30,\ K_{out2(\text{initial})} = 1,\ \alpha_2 = 0.001,\ \beta_2 = 0.01 \tag{68}$$

By using the stability criteria proposed in Section 4, the maximum output scaling-factor of the AMLFCs can be calculated as follows:

$$K_{\max 1} = \frac{L}{2K_eT + K_r\|N_1\|_{2W}} = \frac{0.2}{2(6\cdot 0.01 + 0.1)\cdot 0.1} = 6.25 \tag{69}$$

$$K_{\max 2} = \frac{L}{2K_eT + K_r\|N_2\|_{2W}} = \frac{0.2}{2(1\cdot 0.01 + 0.1)\cdot 0.04} = 22.7 \tag{70}$$

Fig. 10 shows the responses of the tower crane system controlled by the AMLFC versus the RAFC. It shows that both the outputs of the tower crane controlled by the AMLFC achieve steady state values in approximately five seconds, which is much faster compared with those

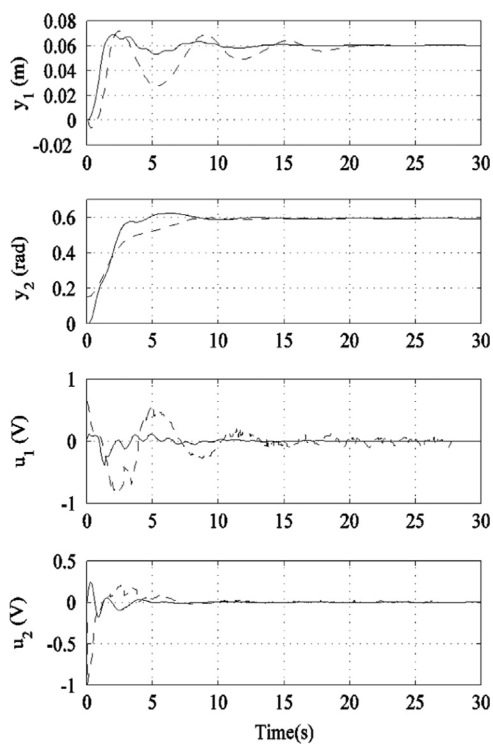

Fig. 10. System response comparison between the AMLFC (solid) and RAFC (dash).

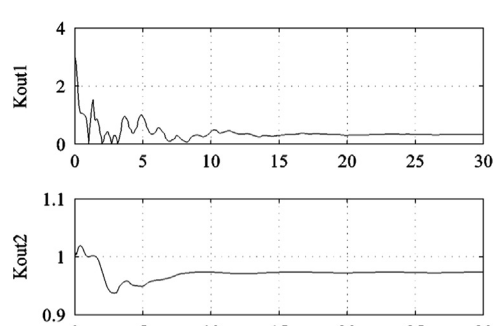

Fig. 11. Output scaling factor of the AMLFCs during control of the tower crane system.

controlled by the RAFC. There is also significantly less oscillation with the AMLFC due to the adaptation of the output scaling factors as shown in Fig. 11, even though the control efforts of the AMLFC are smoother than the control efforts of the RAFC. The overshoots of both outputs of the AMLFC control system are less than ten percents. The adaptation also makes the output responses of the AMLFC follow the desired reference trajectory very closely.

6. Conclusion

A new technique to estimate the dynamic gains of nonlinear systems was presented based on the parameters of the FBFN. Two methods were provided to calculate the L_2 gain and L_∞ gain of FBFN systems by finding the maximum norm value of the local systems and by solving the non-smooth optimal control problem respectively. Based on the proposed methods, an adaptive multilevel fuzzy controller (AMFLC) was proposed with a mechanism to tune the output scaling factor. The first layer of the AMFLC acts as a conventional fuzzy controller, while the second and third layers are used to tune the output scaling factor of the controller by using a fuzzy rule base. Furthermore, a new stability analysis was derived for a nonlinear PI fuzzy control system by using small gain theorem. From the proposed stability analysis, the only design parameter that is needed for a stable fuzzy control system is the maximum output scaling factor of the fuzzy controller. Simulations conducted on a tower crane system provided the superior performance of the proposed AMLFC over the RAFC. With the self-tuning ability of the AMLFC output scaling factor, the control systems stayed within the stable condition. The simulation results showed that the responses of the AMLFC produced a better output transient performance in terms of oscillation and settling time, while the control efforts of the AMLFC were smoother than the control efforts of the RAFC.

References

Arya, R., 2007. Analytical structures and analysis of simplest fuzzy PD controller with asymmetrical/symmetrical, trapezoidal/triangular/singleton output membership function. Int. J. Comput. Cogn. 5, 10–24.

Boubakir, A., Labiod, S., Boudjema, F., 2011. A stable self-tuning proportional-integral-derivative controller for a class of multi-input multi-output nonlinear systems. J. Vib. Control 18, 228–239. http://dx.doi.org/10.1177/1077546311400474.

Bruinsma, N., Steinbuch, M., 1990. A fast algorithm to compute the H∞-norm of a transfer function matrix. Syst. Control Lett. 14, 287–293. http://dx.doi.org/10.1016/0167-6911(90)90049-Z.

Chen, C., Lin, C., Lin, C., 2009. Nonlinear system control using adaptive neural fuzzy networks based on a modified differential evolution. IEEE Trans. Syst. Man Cybern. Part C Appl. Rev. 39, 459–473. http://dx.doi.org/10.1109/TSMCC.2009.2016572.

Chen, G., Ying, H., 1993. Stability analysis of nonlinear fuzzy PI control systems. In: Proceedings of the Third International Conference on Industrial Fuzzy Control and Intelligent Systems. IEEE, Houston, TX, pp. 128–133. http://dx/doi.org/10.1109/IFIS.1993.324200.

Chiang, H.-K., Chu, C.-T., Jhou, Y.-T., 2012. Fuzzy control with fuzzy basis function neural network in magnetic bearing system. In: Proceedings of the International Symposium on Industrial Electronics. IEEE, Hangzhou, pp. 846–851. http://dx/doi.org/10.1109/ISIE.2012.6237199.

Dahleh, M., Verghese, G., 2011. Lectures on dynamic systems and control discrete-time linear state-space models (WWW Document). MIT. ⟨http://ocw.mit.edu/courses/electrical-engineering-and-computer-science/6-241j-dynamic-systems-and-control-spring-2011/readings⟩.

Davis, T.A., Ngo, P.D., Shin, Y.C., 2011. Multi-level fuzzy control of friction stir welding power. Int. J. Adv. Manuf. Technol. 59, 559–567. http://dx.doi.org/10.1007/s00170-011-3522-0.

Desoer, C., Vidyasagar, M., 1975. Feedback Systems: Input–Output Properties. Academic Press, New York.

Gerdts, M., 2008. A nonsmooth Newton's method for control-state constrained optimal control problems. Math. Comput. Simul. 79, 925–936. http://dx.doi.org/10.1016/j.matcom.2008.02.018.

Haj-Ali, A., Ying, H., 2003. Input-output structural relationship between fuzzy controllers using nonlinear input fuzzy sets and PI or PD control. Int. J. Fuzzy Syst., 5.

Haj-Ali, A., Ying, H., 2004. Structural analysis of fuzzy controllers with nonlinear input fuzzy sets in relation to nonlinear PID control with variable gains. Automatica 40, 1551–1559. http://dx.doi.org/10.1016/j.automatica.2004.03.019.

Jiang, H., Yu, J., Zhou, C., 2010. Stable adaptive fuzzy control of nonlinear systems using small-gain theorem and LMI approach. J. Control Theory Appl. 8, 527–532. http://dx.doi.org/10.1007/s11768-010-8035-0.

Lee, C.W., Shin, Y.C., 2001. Construction of fuzzy basis function networks using adaptive least squares method. In: IFSA World Congress and 20th NAFIPS International Conference. IEEE, Vancouver, BC, pp. 2630–2635. http://dx.doi.org/10.1109/NAFIPS.2001.943638.

Lee, C.W., Shin, Y.C., 2003. Construction of fuzzy systems using least-squares method and genetic algorithm. Fuzzy Sets Syst. 137, 297–323. http://dx.doi.org/10.1016/S0165-0114(02)00344-5.

Leng, G., McGinnity, T.M., Prasad, G., 2005. An approach for on-line extraction of fuzzy rules using a self-organising fuzzy neural network. Fuzzy Sets Syst. 150, 211–243. http://dx.doi.org/10.1016/j.fss.2004.03.001.

Li, H., Tong, S., 2003. A hybrid adaptive fuzzy control for a class of nonlinear MIMO systems. IEEE Trans. Fuzzy Syst. 11, 24–34. http://dx.doi.org/10.1109/TFUZZ.2002.806314.

Lin, C.-J., Xu, Y.-J., 2006. A novel genetic reinforcement learning for nonlinear fuzzy control problems. Neurocomputing 69, 2078–2089. http://dx.doi.org/10.1016/j.neucom.2005.09.015.

Mingzhi, H., Jinquan, W., Yongwen, M., Yan, W., Weijiang, L., Xiaofei, S., 2009. Control rules of aeration in a submerged biofilm wastewater treatment process using fuzzy neural networks. Expert Syst. Appl. 36, 10428–10437. http://dx.doi.org/10.1016/j.eswa.2009.01.035.

Mudi, R., Pal, N.R., 1999. A robust self-tuning scheme for PI and PD-type fuzzy controllers. IEEE Trans. Fuzzy Syst. 7, 2–16. http://dx.doi.org/10.1109/91.746295.

Ngo, P.D., Shin, Y.C., 2012. Milling contour error control using multilevel fuzzy controller. Int. J. Adv. Manuf. Technol. 66, 1641–1655. http://dx.doi.org/10.1007/s00170-012-4447-y.

Nikolaou, M., Manousiouthakis, V., 1987. A hybrid approach to nonlinear system theory. In: Proceedings of the 26th IEEE Conference on Decision and Control. IEEE, Los Angeles, CA, pp. 2127–2132. http://dx.doi.org/10.1109/CDC.1987.272934.

Nikolaou, M., Manousiouthakis, V., 1989. A hybrid approach to nonlinear system stability and performance. AIChE J. 35, 559–572. http://dx.doi.org/10.1002/aic.690350406.

Pellegrinetti, G., Bentsman, J., 1996. Nonlinear control oriented boiler modeling – a benchmark problem for controller design. IEEE Trans. Control Syst. Technol. 4, 57–64. http://dx.doi.org/10.1109/87.481767.

Sala, A., 2013. Fuzzy control: from heuristic rules to optimization on thousands of decision variables. In: Seising, R., Trillas, E., Moraga, C., Termini, S. (Eds.), On Fuzziness. Springer-Verlag, Berlin Heidelberg, p. 612.

Schaft, A. van der, 1992. L2-gain analysis of nonlinear systems and nonlinear state-feedback H∞ control. IEEE Trans. Automat. Contr. 37, 770–784. http://dx.doi.org/10.1109/9.256331.

Wang, L., Mendel, J., 1992. Fuzzy basis functions, universal approximation, and orthogonal least-squares learning. IEEE Trans. Neural Netw. 3, 807–814. http://dx.doi.org/10.1109/72.159070.

Woo, Z.-W., Chung, H.-Y., Lin, J.-J., 2000. A PID type fuzzy controller with self-tuning scaling factors. Fuzzy Sets Syst. 115, 321–326. http://dx.doi.org/10.1016/S0165-0114(98)00159-6.

Wu, K., Karkoub, M., Wu, T., 2013. Robust adaptive fuzzy control design for 3-D tower crane with time delayed states. In: Proceedings of the International Conference on Systems, Control and Informatics. Venice, Italy, pp. 193–200.

Xu, C., Shin, Y.C., 2005. Design of a multilevel fuzzy controller for nonlinear systems and stability analysis. IEEE Trans. Fuzzy Syst. 13, 761–778. http://dx.doi.org/10.1109/TFUZZ.2005.859308.

Xu, C., Shin, Y.C., 2011. A self-tuning fuzzy controller for a class of multi-input multi-output nonlinear systems. Eng. Appl. Artif. Intell. 24, 238–250. http://dx.doi.org/10.1016/j.engappai.2010.10.021.
Yang, Y., 2005. Direct robust adaptive fuzzy control (DRAFC) for uncertain nonlinear systems using small gain theorem. Fuzzy Sets Syst. 151, 79–97. http://dx.doi.org/10.1016/j.fss.2004.05.010.
Ying, H., 1994. Practical design of nonlinear fuzzy controllers with stability analysis for regulating processes with unknown mathematical models. Automatica 30, 1185–1195. http://dx.doi.org/10.1016/0005-1098(94)90213-5.